ChemComn

RSCPublishing

COMMUNICATION

Enhancement of 4-electron O_2 reduction by a Cu(II)-pyridylamine complex with a protonated pyridine in the second coordination sphere in water †

Cite this: DOI: 10.1039/x0xx00000x

Received 00th January 2012,
Accepted 00th January 2012

DOI: 10.1039/x0xx00000x

www.rsc.org/

Hiroaki Kotani, Tomomi Yagi, Tomoya Ishizuka, and Takahiko Kojima*

We have synthesised a novel copper(II) complex with a pyridine pendant as a proton relay port for electrocatalytic 4e$^-$ reduction of O_2 in water. The enhancement of the electrocatalytic O_2 reduction by protonation of the pyridine pendant is demonstrated in comparison with a copper(II) complex without the pyridine pendant.

Proton uptake and release at a specific site play a pivotal role in various biological redox-processes performed by metallo-enzymes such as water oxidation in photosynthesis and reduction of dioxygen (O_2) in respiration.[1] In the respiratory chain, chemical reduction of O_2 is coupled with proton pumping across a membrane through hydrogen-bonding network, which is composed of amino acid residues and water molecules.[2] Multinuclear metallo-enzymes such as cytochrome *c* oxidase having a heme iron and a non-heme copper centres in the active site and laccase having a trinuclear copper active site are capable of selective 4e$^-$-reduction of O_2 to water as in eqn (1).[3]

$$O_2 + 4e^- + 4H^+ \longrightarrow 2H_2O \qquad (1)$$

Inspired by those enzymatic reactions, molecular catalysts for 4e$^-$-reduction of O_2 have been developed from the viewpoint not only of biological interests in the reaction mechanism but also of a fuel cell technology as a cathodic reaction.[4] In a recent progress of the molecular design for molecular catalysts, proton relays that is a delivery of protons to O_2-derived species in the second coordination sphere have been recognized to promote reductive O–O bond cleavage, as observed for Fe(III),[6] Co(II),[7] and Ni(II)[8] complexes having acidic protons in the second coordination spheres in organic media. However, the impact of an acidic proton in a second coordination sphere has never been demonstrated in the catalytic O_2 reduction by Cu(II) complexes in water. In this context, a pyridyl group would be appropriate for the proton-accepting site because the protonation of pyridine occur under less acidic conditions (3-methylpyridine in H_2O (293 K): pK_a = 5.68[9a]) in comparison with a carboxylate group (pK_a ~ 4[9b]).

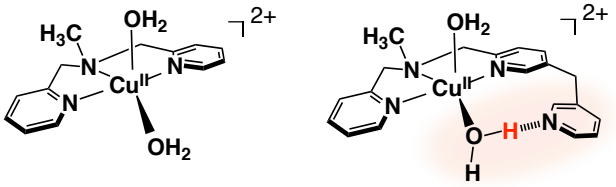

CuNNN **CuNNN-py**

Fig. 1 Chemical structures of Cu^{II} complexes used in this work.

We report herein the development of a new class of Cu(II) complexes with an NNN-type tridentate pincer ligand and an NNN pincer ligand with a non-coordinating pyridine pendant as a distal proton acceptor. The effect of protonation of the non-coordinating pyridine pendant in the second coordination sphere of the Cu(II) complex on the electrocatalytic O_2 reduction was investigated in comparison with that by a Cu complex without the pyridine pendant as a reference.

The syntheses of Cu(II) complexes having tridentate ligands (**NNN** and **NNN-py**)[10] in Fig. 1 were accomplished by the synthetic procedures described in experimental section in the ESI†. The pyridine pendant was introduced to the 5-position of one of chelating pyridine rings linked *via* one methylene group at the 3-position of the pendant to avoid chelation. In the ESI-TOF-MS spectrum, **CuNNN-py** exhibited a peak cluster assigned to a mononuclear species at *m*/*z* = 386.14 (calcd. for $[Cu(F)(\mathbf{NNN\text{-}py})]^+$: 386.10) as shown in Fig S1 in the ESI†.[11] X-ray crystallography revealed that the Cu(II) complex with the **NNN-py** ligand showed a dimeric structure as $[Cu(BF_4)_2(\mathbf{NNN\text{-}py})]_2$ ($(\mathbf{CuNNN\text{-}py})_2$), accompanying mutual coordination of the pendant pyridine (N4), as depicted in Fig. 2. In the crystal, each Cu(II) centre bound with two BF_4^- ions at the axial positions (Fig S2 in the ESI†).

In order to investigate the structure of **CuNNN-py** in aqueous solution, further characterization of **CuNNN-py** in

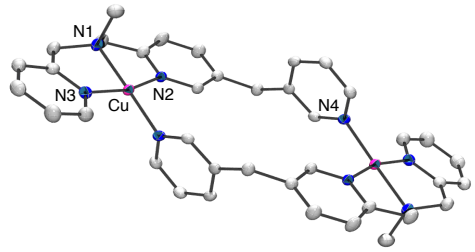

Fig. 2 An ORTEP drawing of the cation moiety of (**CuNNN-py**)$_2$ using 50% probability thermal ellipsoids with numbering scheme for the heteroatoms. Hydrogen atoms and axially bound BF_4^- ions are omitted for clarity (see Fig. S2 in the ESI†).

water was made by UV-vis and electron spin resonance (ESR) spectroscopies. UV-vis measurements on (**CuNNN-py**)$_2$ in various concentrations (1.02 – 14.7 mM) at pH 6.6 in water allowed us to observe blue shifts of an absorption band derived from a d-d transition from 660 nm to 608 nm (Fig S3a in the ESI†). The blue shifts were analyzed to determine the formation constant (K = 79 M^{-1}) of a dinuclear Cu(II) complex with **NNN-py** as found in the crystal structure from a mononuclear Cu(II) complex in water on the basis of a plot of the wavelength at absorption maximum *vs.* the total concentration of Cu(II) complexes with **NNN-py** (eqn S1 and Fig S3c in the ESI†). Therefore, (**CuNNN-py**)$_2$ should dissociate to be a mononuclear species in aqueous solution at lower concentrations. In sharp contrast to the results at pH 6.6, no shift was observed for the absorption band at pH 4.2, indicating protonation of non-coordinating pyridine should inhibit the dimer formation (Fig S3b in the ESI†). These results strongly support that (**CuNNN-py**)$_2$ exists as a mononuclear form, **CuNNN-py** at pH 6.7, and that with a protonated pendant pyridine, *i.e.* **CuNNN-pyH**$^+$, at pH 4.2 in aqueous solution.

ESR measurements on **CuNNN-py** in H_2O at pH 4.2 and pH 6.7 allowed us to observe identical signals at g_{iso} = 2.15, showing a relatively small $A_{//}$ value (70 G), as shown in Fig S4a in the ESI†. In the case of a Cu(II) complex with **NNN** as a ligand (**CuNNN**, Fig. 1), ESR signals were also observed at g_{iso} = 2.14, accompanying hyperfine splitting with an $A_{//}$ value of 70 G (Fig S4c in the ESI†). Compared with that (150 G) of (**CuNNN-py**)$_2$ in the solid state,[3a] the $A_{//}$ values were much smaller in aqueous media at both pH 4.2 and 6.7. These results indicate that a five-coordinated trigonal bipyramidal structure is preferred for **CuNNN-py**, **CuNNN-pyH**$^+$ and **CuNNN** in H_2O. In all cases, regardless of pH values of solutions, the Cu(II) centres probably accompany coordination of two water molecules besides the corresponding tridentate ligand, judging from the small $A_{//}$ value.[12] As for **CuNNN-py**, a trigonal bipyramidal structure with two aqua ligands was optimized by DFT calculations, suggesting that the pendant pyridine can locate nearby one of the aqua ligands to form intramolecular hydrogen bonding to be stabilized (Fig S5 in the ESI†).

In order to clarify the redox properties of the Cu(II) complexes, we conducted electrochemical measurements, including cyclic voltammetry (CV) and differential-pulse voltammetry (DPV) in aqueous solutions in the presence of 0.1 M KNO_3 as an electrolyte at 298 K under Ar. One-electron reduction potential (E_{red}, V *vs.* SCE) of **CuNNN-pyH**$^+$ were determined to be –0.24 V at pH 4.2 and that of **CuNNN-py** to be –0.25 V at pH 6.7 at 298 K in water, which were slightly higher than those of **CuNNN** (–0.31 V at pH 4.2 and pH 6.7) as shown in Fig. 3a,b. Besides the pK_a value (pK_a ~ 5.7) of the pendant pyridine moiety,[9] the reduction potentials of **CuNNN-py** showed no pH-dependence. This result indicates that the protonation of the pendant pyridine does not affect the E_{red} value under the conditions of electrochemical measurements. In addition, no catalytic current was observed in each case under Ar.

In contrast to the results under Ar, CV traces of **CuNNN-py** and **CuNNN** under O_2 exhibited catalytic currents due to the electrochemical O_2 reduction at around –0.4 V (Fig. 3c,d and Fig S6 in the ESI†). To confirm the stoichiometry of the electrochemical O_2 reduction by the Cu(II) complexes in water, the amount of H_2O_2 as a 2e$^-$-reduced product of O_2 was measured by iodometric titration experiments as described in the experimental section in the ESI†. The yields of H_2O_2 were determined to be 37% at pH 4.2 and 67% at pH 6.7 for **CuNNN-py**, 63% at pH 4.2 and 61% at pH 6.7 for **CuNNN**, respectively (Fig S7 in the ESI†).

The rotating ring-disk voltammetry (RRDV) was also employed for a quantitative detection of the produced H_2O_2: only H_2O_2 generated at the disk electrode is oxidized by the Pt ring disk to show ring current, on the contrary, H_2O is not oxidized and thus no ring current is observed. The H_2O_2 yields (H_2O_2%) were given by eqn (2),[13,14] where N is the theoretical collection efficiency and i_D and i_R is the disk and ring currents, respectively.

$$H_2O_2\% = \frac{200 i_R/N}{i_D + i_R/N} \qquad (2)$$

The H_2O_2 yields were determined to be 41% at pH 4.2 and 77% at pH 6.7 for **CuNNN-py**, 75% at pH 4.2 and 76% at pH 6.7 for **CuNNN** by RRDV measurements, respectively, as shown in Fig 4, under the same conditions as those of CV and DPV experiments. In the case of **CuNNN-pyH**$^+$ at pH 4.2, i_R due to the oxidation of H_2O_2 is smaller than those observed in other cases. The results of iodometric and RRDV measurements are consistent as can be seen in Table 1 to confirm the selectivity (4e$^-$ or 2e$^-$) in electrochemical O_2 reduction by **CuNNN-py** and **CuNNN**; the 4e$^-$-reduction of O_2 is dominant for **CuNNN-pyH**$^+$ under acidic conditions, where the pendant pyridine is protonated.

Assuming the remaining electrons could be consumed for

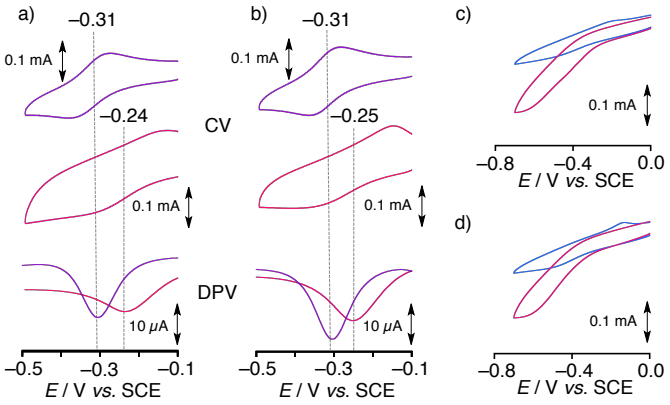

Fig. 3 Cyclic voltammograms and differential pulse voltammograms of **CuNNN** (purple) **CuNNN-py** (pink) at (a) pH 4.2 and (b) pH 6.7 in H_2O at 298 K under Ar. Cyclic voltammograms of **CuNNN-py** at (c) pH 4.2 and (d) pH 6.7 under Ar (blue) and O_2 (pink).

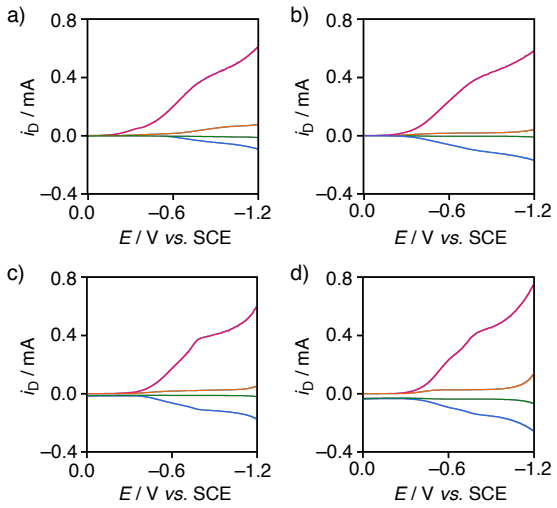

Fig. 4 Rotating ring-disk voltammograms for (a) **CuNNN-pyH**$^+$ at pH 4.2, (b) **CuNNN-py** at pH 6.7, (c) **CuNNN** at pH 4.2, and (d) **CuNNN** at pH 6.7 in 0.1 M KNO_3 bubbled with 1 atm O_2 or 1 atm Ar at 298 K. i_D of O_2 (pink), i_R of O_2 (blue), i_D of Ar (orange), i_R of Ar (green). E_R = 1.0 V *vs.* SCE, 20 mV/s, 400 rpm.

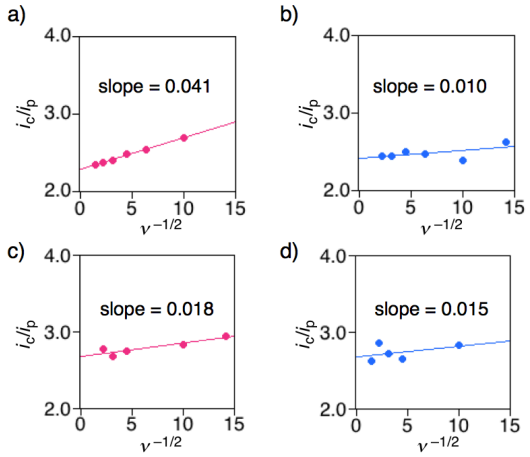

Fig. 5 Plots of the ratio of the catalytic current, i_c, to the blank peak current, i_p, *vs.* $\nu^{-1/2}$ (a) **CuNNN-pyH**$^+$ at pH 4.2, (b) **CuNNN-py** at pH 6.7, (c) **CuNNN-py** at pH 4.2, (d) **CuNNN** at pH 6.7. Conditions: [Cu complex] = 0.5 mM, 298 K.

4e$^-$-reduction of O_2 to produce H_2O, the number of electrons transferred in the O_2 reduction is given as follows: For **CuNNN-py**, 3.18 e$^-$ at pH 4.2 (**CuNNN-pyH**$^+$) and 2.46 e$^-$ at pH 6.7 (**CuNNN-py**); for **CuNNN**, 2.52 e$^-$ at pH 4.2 and 2.48 e$^-$ at pH 6.7 as summarized in Table 1.[15] The stoichiometry of the O_2 reduction was also estimated by the consumed amount of a one-electron reductant, methyl viologen radical cation ($MV^{\bullet+}$), in the UV-vis spectroscopic measurements under O_2-limiting conditions (4[O_2] < [$MV^{\bullet+}$]; [O_2] = 0.013 mM, [$MV^{\bullet+}$] = 0.2 mM) (Fig S8 in the ESI†).[5b,16] As a result, 0.038 mM of $MV^{\bullet+}$ (n_{cat} = 2.92 e$^-$) was consumed under O_2 (0.013 mM) in the presence of **CuNNN-pyH**$^+$ at pH 4.2 in H_2O. The amount of the reductant consumed exceeded that required $MV^{\bullet+}$ (0.026 mM) for the 2e$^-$-reduction of O_2. This result is in good agreement with the number of electrons (n_{cat} = 3.18 e$^-$) obtained by the RRDV experiment, supporting further reduction of O_2 to afford H_2O as the 4e$^-$-reduced product.

Table 1 One-electron reduction potentials (E_{red}), H_2O_2 yields determined by iodometry and RRDV, number of electrons transferred (n_{cat}), and reaction rate constants of catalytic O_2 reduction under O_2 (k_{cat}) of **CuNNN-py** and **CuNNN** in pH 4.2 and 6.7 aqueous solution at 298 K.

	CuNNN-py		**CuNNN**	
	pH 4.2	pH 6.7	pH 4.2	pH 6.7
E_{red}, V *vs.* SCE	–0.24	–0.25	–0.31	–0.31
H_2O_2 yield by iodometry[a]	37%	67%	63%	61%
H_2O_2 yield by RRDV	41%	77%	75%	76%
n_{cat}	3.18	2.46	2.52	2.48
k_{cat}, h^{-1} [b]	4.65	0.46	1.45	1.02

a Bulk electrolysis at –0.8 V for 70 sec.
b k_{cat} values in eqn (3) were calculated by using n_{cat} values.

$$\frac{i_c}{i_p} = 2.24 n_{cat} \left(\frac{k_{cat} RT}{nF\nu} \right)^{1/2} \quad (3)$$

The reaction rate constants of catalytic O_2 reduction (k_{cat}) were determined from the slope of the plot (i_c/i_p *vs.* $\nu^{-1/2}$) according to eqn (3), where i_c is catalytic peak current, i_p is non-catalytic peak current, n_{cat} is the number of electrons transferred, n is the number of electrons transferred under the non-catalytic conditions, F is the Faraday constant (96485 C mol^{-1}).[17,18] Thus, k_{cat} values were determined to be 4.65 h^{-1} at pH 4.2 and 0.46 h^{-1} at pH 6.7 for **CuNNN-pyH**$^+$ and **CuNNN-py**, respectively as shown in Fig. 5. In contrast to the case of **CuNNN-py**, no pH-dependence of k_{cat} was observed in the case of **CuNNN** (1.45 h^{-1} at pH 4.2 and 1.02 h^{-1} at pH 6.7). These electrochemical data are summarized in Table 1. As can be seen in Table 1, the k_{cat} value of **CuNNN-pyH**$^+$ at pH 4.2 is highest in the electrocatalytic O_2 reduction experiments. Thereby, protonation of non-coordinated protonated pyridine of **CuNNN-py** in the second coordination sphere has been demonstrated to exhibit significant contribution to the promotion of the catalytic 4e$^-$-reduction of O_2 in acidic water.

In order to shed light on the reaction intermediate, DFT calculations were conducted on O_2-bound species of **CuNNN-pyH**$^+$. An optimized structure was obtained for a hydroperoxo intermediate with hydrogen bonding between the pendant **pyH**$^+$ and the distal oxygen in the Cu^{II}-OOH moiety as shown in Fig 6.[19] This hydrogen-bonding interaction is expected to facilitate reductive O–O bond cleavage to proceed the 4e$^-$-reduction of O_2 as shown in Scheme 1.[6]

In contrast, catalytic 4e$^-$-reduction of O_2 by **CuNNN-py** was less favourable at pH 6.7 than that of **CuNNN-pyH**$^+$ at pH 4.2, as reflected on the higher yield of H_2O_2 (see Table 1). The superiority of the 2e$^-$ reduction affording H_2O_2 to the 4e$^-$ reduction at pH 6.7 should stem from the lack of the hydrogen bonding in the putative Cu(II)-hydroperoxo intermediate, which should be important for further reduction involving the reductive O-O cleavage.

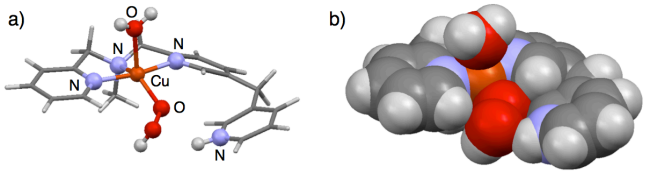

Fig. 6 (a) A DFT-optimized structure of the hydroperoxo species of **CuNNN-pyH**$^+$. (b) Space-filling representation.

Scheme 1

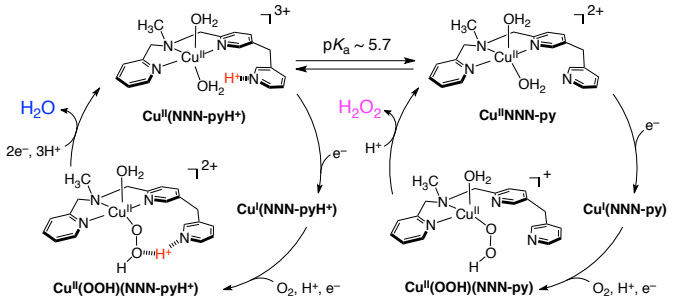

Proposed mechanisms of O_2 reduction by **CuNNN-py** (pH 6.7) and **CuNNN-pyH**$^+$ (pH 4.2) are depicted in Scheme 1. The mechanisms can be switched by protonation of the pendant pyridine. The corresponding mononuclear Cu(II) complexes are reduced electrochemically to produce reactive Cu(I) complexes, which should be ready for the reaction with O_2 to afford Cu-O_2 species.[3b,20] Following proton-coupled electron-transfer (PCET) reduction of Cu-O_2 species forms Cu(II)-OOH complexes as intermediates. The Cu(II)-OOH species with **NNN-pyH**$^+$ is more activated toward further PCET reduction to form water preferentially.[5b] On the contrary, the Cu(II)-OOH species with **NNN-py** or **NNN** may undergo protonation of the hydroperoxo ligand to release H_2O_2, rather than H_2O.[21]

In conclusion, we have synthesized a Cu(II) complex with NNN-pincer ligand with a non-chelating pendant pyridine as a proton acceptor in the second coordination sphere. The proton trapped in the second coordination sphere surely promotes catalytic proton-coupled 4e$^-$ reduction of O_2, as confirmed by the electrochemical experiments in comparison with the corresponding Cu(II) complex without the pendant pyridine.

This work was partially supported by Grants-in-Aid (Nos. 25109507, 25107508 and 24245011) from the Japan Society of Promotion of Science (JSPS, MEXT) and the Mitsubishi Foundation.

Notes and references

Department of Chemistry, Faculty of Pure and Applied Sciences, University of Tsukuba, 1-1-1 Tennoudai, Tsukuba, Ibaraki 305-8571, Japan. E-mail: kojima@chem.tsukuba.ac.jp; Fax: +81-29-853-4323

† Electronic Supplementary Information (ESI) available: crystallographic data of (**CuNNN-py**)$_2$ in the CIF format, ESI-TOF-MS, UV-vis, and ESR spectra, DFT-optimized structure of [Cu(**NNN-py**)$(H_2O)_2]^{2+}$, CV data, and Cartesian coordinates for DFT-optimized structures. CCDC 1058367. See DOI: 10.1039/c000000x/

1 S. Ferguson-Miller and G. T. Babcock, *Chem. Rev.*, 1996, **96**, 2889−2907.

2 (*a*) B. E. Ramirez, B. G. Malmstromt, J. R. Winkler and H. B. Gray, *Proc. Natl. Acad. Sci. U. S. A.*, 1995, **92**, 11949–11951; (*b*) A. Namslauer, A. S. Pawate, R. B. Gennis and P. Brzezinski, *Proc. Natl. Acad. Sci. U. S. A.*, 2003, **100**, 15543–15547.

3 (*a*) E. I. Solomon, U. M. Sundaram and T. E. Machonkin, *Chem. Rev.*, 1996, **96**, 2563−2605; (*b*) L. M. Mirica, X. Ottenwaelder and T. D. P. Stack, *Chem. Rev.*, 2004, **104**, 1013−1045; (*c*) E. Kim, E. E. Chufán, K. Kamaraj and K. D. Karlin, *Chem. Rev.*, 2004, **104**, 1077−1133; (*d*) J. P. Collman, R. Boulatov, C. J. Sunderland and L. Fu, *Chem. Rev.*, 2004, **104**, 561−588.

4 (*a*) C. C. L. McCrory, A. Devadoss, X. Ottenwaelder, R. D. Lowe, T. D. P. Stack and C. E. D. Chidsey, *J. Am. Chem. Soc.*, 2011, **133**, 3696–3699; (*b*) P. Agbo, J. R. Heath and H. B. Gray, *J. Am. Chem. Soc.*, 2014, **136**, 13882–13887. (*c*) D. J. Wasylenko, C. Rodríguez, M. L. Pegis and J. M. Mayer, *J. Am. Chem. Soc.*, 2014, **136**, 12544–12547.

5 (*a*) A. Wada, M. Harata, K. Hasegawa, K. Jitsukawa, H. Masuda, M. Mukai, T. Kitagawa and H. Einaga, *Angew. Chem. Int. Ed.* 1998, **37**, 798–799; (*b*) S. Kakuda, R. L. Peterson, K. Ohkubo, K. D. Karlin and S. Fukuzumi, *J. Am. Chem. Soc.*, 2013, **135**, 6513–6522.

6 (*a*) C. T. Carver, B. D. Matson and J. M. Mayer, *J. Am. Chem. Soc.*, 2012, **134**, 5444–5447; (*b*) B. D. Maston, C. T. Carver, A. V. Ruden, J. Y. Yang, S. Raugei and J. M. Mayer, *Chem. Commun.*, 2012, **48**, 11100−11102; (*c*) M. L. Rigsby, D. J. Wasylenko, M. L. Pegis, J. M. Mayer, *J. Am. Chem. Soc.*, 2015, **137**, 4296–4299.

7 (*a*) R. McGuire Jr, D. K. Dogutan, T. S. Teets, J. Suntivich, Y. Shao-Horn and D. G. Nocera, *Chem. Sci.*, 2010, **1**, 411–414; (*b*) J. D. Baran, H. Grönbeck and A. Hellman, *J. Am. Chem. Soc.*, 2014, **136**, 1320–1326

8 J. Y. Yang, R. M. Bullock, W. G. Dougherty, W. S. Kassel, B. Twamley, D. L. DuBois and M. R. DuBois, *Dalton Trans.,* 2010, **39**, 3001–3010.

9 (*a*) L. Joris and R. Schleyer, *Tetrahedron*, 1968, **24**, 5991–6005; (*b*) P. W. Atkins, T. L. Overton, J. P. Rourke, M. T. Weller and F. A. Armstrong, *Shriver & Atkins' Inorganic Chemistry, 5th ed.*; Oxford University Press: New York, 2010, pp. 115.

10 Abbreviations: **NNN**: *N*-methyl-*N*,*N*-bis(2-pyridylmethyl)amine, and **NNN-py**: *N*-methyl-*N*-(2-pyridylmethyl)-*N*-{5-(3-pyridylmethyl)-2-pyridylmethyl}amine.

11 The coordinated fluoride anion (F^-) was presumably derived from decomposition of the BF_4^- anion in the ionization process of ESI-TOF-MS measurements. See: (*a*) J. Ackermann, F. Meyer and H. Pritzkow, *Inorg. Chim. Acta*, 2004, **357**, 3703−3711; (*b*) H. Kotani, S. Kaida, T. Ishizuka, M. Sakaguchi, T. Ogura, Y. Shiota, K. Yoshizawa, T. Kojima. *Chem. Sci.* 2015, **6**, 945–955.

12 C.-C. Su , W.-S. Lu, T.-Y. Hui, T.-Y. Chang, S.-L. Wang and F.-L. Liao, *Polyhedron*, 1993, **12**, 2249−2259.

13 O. Antoine and R. Durand, *J. Appl. Electrochem.*, 2000, **30**, 839–844.

14 Y. Feng, T. Heb, and N. Alonso-Vantea, *Electrochimica Acta*, 2009, **54**, 5252–5256.

15 I. Roche, E. Chaînet, M. Chatenet and J. Vondrák, *J. Phys. Chem. C*, 2007, **111**, 1434–1443.

16 Determination of the stoichiometry of O_2 reduction by one-electron reductants under O_2-limiting conditions, see: (*a*) D. J. Wasylenko, C. Rodríguez, M. L. Pegis and J. M. Mayer, *J. Am. Chem. Soc.*, 2014, **136**, 12544–12547; (*b*) S. Fukuzumi, H. Kotani, H. R. Lucas, K. Doi, T. Suenobu, R. L. Peterson and K. D. Karlin, *J. Am. Chem. Soc.* 2010, **132**, 6874–6875.

17 A. J. Bard, and L. R. Faulkner, *Electrochemical Methods: Fundamentals and Applications, 2nd ed.*; Wiley: New York, 2001.

18 E. S. Rountree, B. D. McCarthy, T. T. Eisenhart and J. L. Dempsey, *Inorg. Chem.*, 2014, **53**, 9983–10002.

19 It should be noted that this structure only afforded optimized structure with **pyH**$^+$ hydrogen bonding among any O_2-bound Cu complexes.

20 (*a*) E. A. Lewis and W. B. Tolman, *Chem. Rev.*, 2004, **104**, 1047−1076; (*b*) L. Q. Hatcher and K. D. Karlin, *J. Biol. Inorg. Chem.*, 2004, **9**, 669–683; (*c*) J. H. Lee, R. L. Peterson, K. Ohkubo, I. Garcia-Bosch, R. A. Himes, J. Woertink, C. D. Moore, E. I. Solomon, S. Fukuzumi and K. D. Karlin, *J. Am. Chem. Soc.*, 2014, **136**, 9925–9937.

21 R. L. Peterson, J. W. Ginsbach, R. E. Cowley, M. F. Qayyum, R. A. Himes, M. A. Sieger, C. D. Moore, B. Hedman, K. O. Hodgson, S. Fukuzumi, E. I. Solomon and K. D. Karlin, *J. Am. Chem. Soc.*, 2013, **135**, 16454–16467.

